

# Synthesis of Magnetite Fe<sub>3</sub>O<sub>4</sub> Nanoparticles for the Removal of Divalent Nickel Ions from Aqueous Media

Prapti P. Warbhe<sup>1</sup>, Rakesh M. Naktode<sup>2</sup>, Mamta R. Lanjewar<sup>3</sup>

<sup>1</sup>Research Scholar, Department of Chemistry, RTM Nagpur University, Nagpur, Maharashtra, India.

<sup>2</sup>Assistant Professor, Dada Ramchand Bakharu Sindhu Mahavidyalaya, Nagpur, Maharashtra, India.

<sup>3</sup>Professor, Department of Chemistry, RTM Nagpur University, Nagpur, Maharashtra, India.

## Abstract

One of the environmental issues of the twenty-first century is the heavy metal pollution of water. Numerous techniques for eliminating heavy metal ions from water have been thoroughly researched. Since magnetite nanoparticle-based nanomaterials are widely used to remove heavy metals, this work examined the use of Fe<sub>3</sub>O<sub>4</sub> nanoparticles to remove the Ni(II) ion from an aqueous solution. Utilising FTIR, SEM, and XRD methods, the synthesised nanoparticle was described. The results of the batch studies demonstrated that Ni(II) may be efficiently extracted from an aqueous solution using magnetite nanoparticles. Ni(II) was removed in large proportion (94.24%) from its aqueous solution at pH = 6, starting with a with a metal ion concentration of 40 ppm, a nanoparticle dose of 0.4 g, a contact duration of 35 min, and a rpm of 180. The mechanism of Ni(II) elimination was determined by applying the kinetic models. This finding might be helpful for removing Ni(II) ions from wastewater.

**Keywords:** Fe<sub>3</sub>O<sub>4</sub> Nanoparticle, Ni(II) ion, Freundlich Isotherm, Pseudo Second Order, Wastewater.

## 1. Introduction

As the global economy has grown, environmental degradation has become a challenging issue that no nation can escape[1]. Pollution issues are a common topic in the news, especially in rapidly developing nations. For example, wastewater from several industries such as battery production, tanneries, chemical manufacturing, mining, etc. pollutes rivers and land because it contains a lot of heavy metal ions[2]. Toxic metal ion contamination of water, specifically Hg(II), Pb(II), Cr(III), Cr(VI), Ni(II), Co(II), Cu(II), Cd(II), Ag(I), As(V) and As(III) has rapidly grown into a serious environmental and public health concern[3]. Nickel(II) is one of these heavy metal ions that is hazardous and non-biodegradable in wastewater[4]. Industrial operations include galvanization, smelting, mining, dyeing, battery production, steel plants, and metal finishing are the primary causes of nickel pollution. Several illnesses, including cancer, renal oedema, skin dermatitis, and gastrointestinal disorders, can arise when the amount of nickel(II) is higher than the usual level[5]. For chemists and environmentalists, removing the aforementioned heavy metal ions has become a major topic. Many techniques have been employed, including cementation, resins, chemical precipitation, ion exchange, electrolysis, reverse osmosis, and liquid-liquid extraction[1]. Each of them has certain drawbacks, including high costs, complexity, limited efficiency, and secondary waste[1,6,7]. Because of their exceptional properties, nano adsorbents have recently gained widespread

interest[1,8,9]. Fe<sub>3</sub>O<sub>4</sub> nanoparticles are a novel class of nanomaterials characterised by their high saturation, high magnetization, large surface area, super Para magnetism, uniform particle size distribution, chemical stability, enrichment, ease of recycling, low toxicity, and affordability. They have been extensively employed in the treatment of wastewater[10]. Due to their large surface to volume ratio, which produces a better adsorption capacity for metal removal, magnetite (Fe<sub>3</sub>O<sub>4</sub>) nanoparticles have been used in this experiment to remove heavy metals[11]. Additionally, iron oxide nanoparticles (Fe<sub>3</sub>O<sub>4</sub>) for the removal of heavy metals have been approved by the USA Food and Drug Administration[11]. We synthesised magnetite (Fe<sub>3</sub>O<sub>4</sub>) nanoparticles by using the sol-gel method, and we investigated their characterization and nickel-based water treatment.

## 2. Material and method

### 2.1 Material

Ethylene glycol (C<sub>2</sub>H<sub>6</sub>O<sub>2</sub>) (A R grade) and ferric nitrate [Fe (NO<sub>3</sub>)<sub>3</sub>.9H<sub>2</sub>O] (MERCK INDIA), nickel sulphate (A R grade), dimethyl glyoxime, bromine water, and ammonia were brought from Merk, India. Aqueous solutions were prepared using double-distilled water. Since all of the reagents were analytical grade, no further purification was needed.

### 2.2 Preparation of magnetite nanoparticle

The following describes the manufacturing of ferric oxide nanoparticles:

Firstly, ferric nitrate was combined with 100 ml of ethylene glycol and heated to 40 °C while being vigorously stirred for an hour in order to form a sol. After that, the brown colour solution was heated steadily to 80 °C till a dark brown colour gel was created. This gel was aged for four hours and then dried at 120 °C for five hours. The final xerogel was annealed at a particular temperature while being kept under vacuum. Ultimately, magnetite nanoparticles were successfully generated. The synthesised Fe<sub>3</sub>O<sub>4</sub> nanoparticles were washed in acetone and ethanol to enhance their magnetic properties.

## 3. Result and discussion

### 3.1 FTIR Analysis

Fe<sub>3</sub>O<sub>4</sub> FTIR tests were performed to identify the metal oxygen bond, as shown in Figure 1. Adsorption bands at 1641.56 cm<sup>-1</sup> and 3565.14 cm<sup>-1</sup> correspond to the C=O and O-H modes, respectively. The adsorption band at 428.23 cm<sup>-1</sup> and 540 cm<sup>-1</sup> displays the vibration of Fe-O[12].

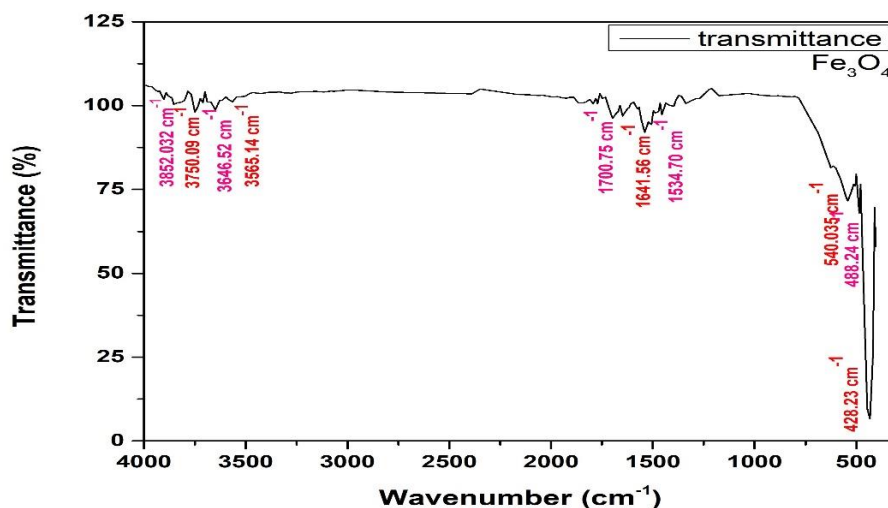


Figure 1: FTIR of Fe<sub>3</sub>O<sub>4</sub>

### 3.2 XRD Analysis

The diffraction peaks at  $2\theta = 19^\circ, 30^\circ, 36^\circ, 43^\circ, 54^\circ, 57^\circ, 63^\circ, 71^\circ, 75^\circ,$  and  $79^\circ$  can be attributed to the  $\text{Fe}_3\text{O}_4$  (PCPDF # 391346) planes (111), (220), (311), (400), (422), (511), (440), (620), (533), and (444). This is demonstrated in Figure 2. The Scherrer formula is used to determine the crystallite size of a nanoparticle.

$$D = \frac{K \cdot \lambda}{\beta \cdot \cos \theta}$$

The variables  $K, \lambda, \beta,$  and  $\theta$  represent the dimensionless form factor, FWHM, x-ray wavelength, and Bragg angle, respectively. 14.43 nm is the average crystallite size of  $\text{Fe}_3\text{O}_4$ .

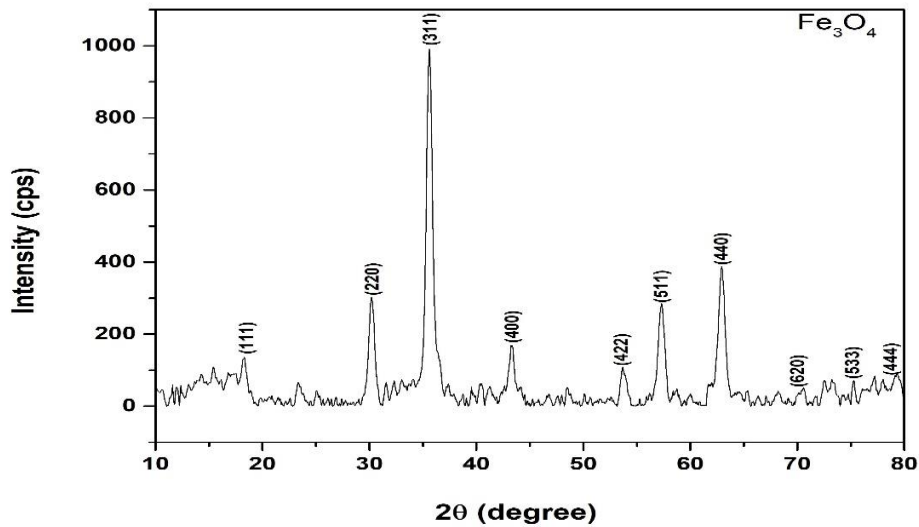


Figure 2: XRD spectra of  $\text{Fe}_3\text{O}_4$

### 3.3 SEM Analysis

The similar pictures of the  $\text{Fe}_3\text{O}_4$  nanoparticles at  $400^\circ\text{C}$  are shown in Figures 3 and 4. Evidence suggests that xerogel is the cause of the nanoparticle aggregation.

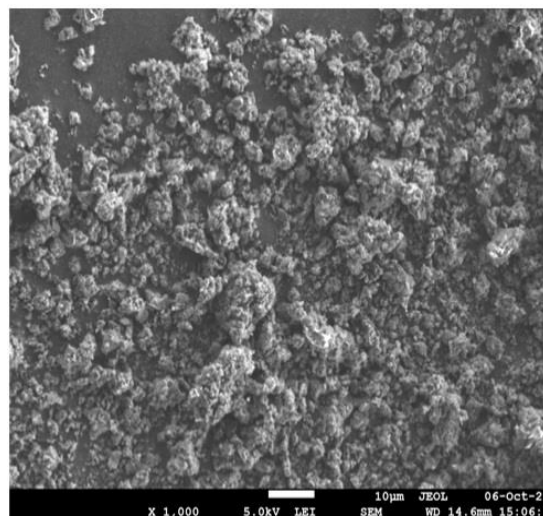


Figure 3: SEM of  $\text{Fe}_3\text{O}_4$

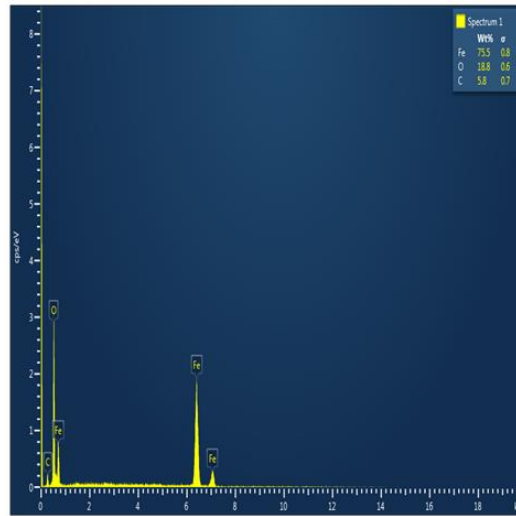


Figure 4: Fe<sub>3</sub>O<sub>4</sub> EDX image of

#### 4. Batch study

In order to comprehend the efficient adsorption characteristics of nickel ions onto Fe<sub>3</sub>O<sub>4</sub>, batch experiments were conducted utilising optimised settings, including starting Ni(II) concentrations ranging from 10 to 100 ppm, adsorbent doses of 0.1 to 1 g, contact times of 5 to 50 min, and working pH values of 4 to 8. Follows were the standard procedure. After adding the desired amount of synthetic Fe<sub>3</sub>O<sub>4</sub> nano adsorbents to a 50 ml Erlenmeyer flask holding a 25 ml solution of Ni(II) at a predetermined concentration, the sample solution was shaken for a certain amount of time at 180 rpm on a NAVYUG (India) rotary shaker. The material was then filtered through Whatman filter paper no. 40, and the residual Ni(II) concentration was determined at 443 nm using a Shimadzu UV/Vis spectrophotometer. The proportion of adsorption and the capacity of adsorption were determined (equations 1 and 2) for fallows[13,14].

$$R\% = \frac{C_0 - C_e}{C_0} \times 100 \quad (1)$$

$$q_e = (C_0 - C_e) \times \frac{V}{m} \quad (2)$$

where V is the volume (ml) of the solution taken, W (g) is the mass of the adsorbent utilised, C<sub>0</sub> is the initial concentration in the metal ion solution (mg/L), and C<sub>e</sub> is the final metal ion concentration in the aqueous solution after adsorption (mg/L). Where q<sub>e</sub> is the maximal adsorption capacity and R% is the adsorption percentage.

#### 4.1 Adsorbate preparation

NiSO<sub>4</sub> (0.492 g) was dissolved in 1000 ml of double-distilled water to make a stock solution of Ni(II). Using Fe<sub>3</sub>O<sub>4</sub> as an adsorbent, adsorption studies were carried out to examine the impact of adsorption parameters on Ni(II), including starting concentration, adsorbent dosage, contact time, and pH of the solution absorption.

### 5. Batch experiments

#### 5.1 Effect of initial concentration on percentage removal of Ni(II) using Fe<sub>3</sub>O<sub>4</sub> nanoparticle as adsorbent

Using a fixed dose of synthetic nanoFe<sub>3</sub>O<sub>4</sub> (0.5 g) and a contact time of 90 min and a pH of 6-7, the adso-

ption experiment was conducted with different concentrations of Ni(II) ions (10 to 100 ppm). Figure 5 diagrammatically illustrates how the concentration of Ni(II) affects the percentage removal fluctuation. When the concentration was low, the proportion of Ni(II) ions removed by nanoFe<sub>3</sub>O<sub>4</sub> was found to be high and to progressively increase.

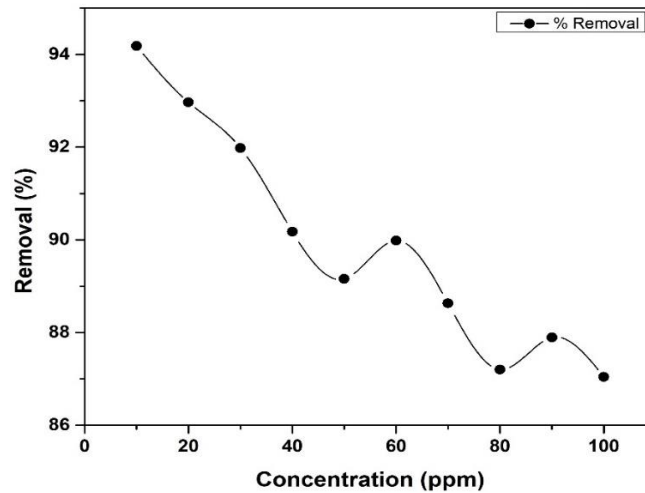


Figure 5: Effect of initial concentration

### 5.2 Effect of adsorbent dosage on percentage removal of Ni(II) using Fe<sub>3</sub>O<sub>4</sub> nanoparticle as adsorbent

When determining adsorption capacity, the dose of the adsorbent is a crucial factor. Better adsorption occurs as a result of an increase in the adsorbent dosage, which also increases the number of adsorbent sites accessible for Ni(II) metal ions. The current investigation involved varying the dose of adsorbent in Ni(II) solutions from 0.1 to 0.55 g while maintaining constants for rpm and metal ion concentration. A maximum removal rate of 94.40% was achieved with an optimal dosage of 0.4 g. Figure 6 shows that as the dose of Fe<sub>3</sub>O<sub>4</sub> is increased, the percentage elimination of nickel metal increases. nanoparticle and stayed almost unchanged once the ideal dosage of 0.4 g was chosen to move forward with the wastewater treatment process. This technique is sometimes referred to as optimisation based on one factor at a time, in which one parameter is changed while the others remain unchanged[15,16].

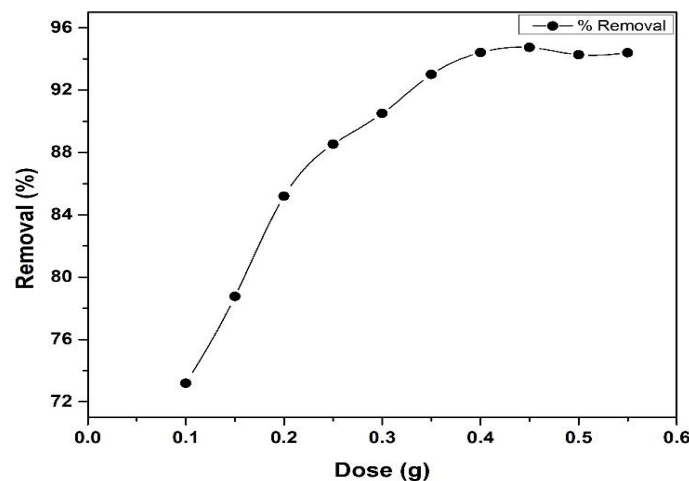


Figure 6: Effect of adsorbent dosage

### 5.3 Effect of constant time on percentage removal of Ni(II) using Fe<sub>3</sub>O<sub>4</sub> nanoparticle as adsorbent

By changing the constant duration from 5 to 50 min with an optimised Fe<sub>3</sub>O<sub>4</sub> dosage and beginning metal ion concentration, the maximum dye removal effectiveness of synthetic and industrial effluent was investigated. When the contact duration was extended from 5 to 35 min, the Ni(II) removal efficiency rose quickly and stayed constant after that. Using synthetic effluent for 35 minutes, a 94% clearance efficiency of Ni(II) was achieved. Therefore, ideal figure 7 was produced with a constant time of 35 min.

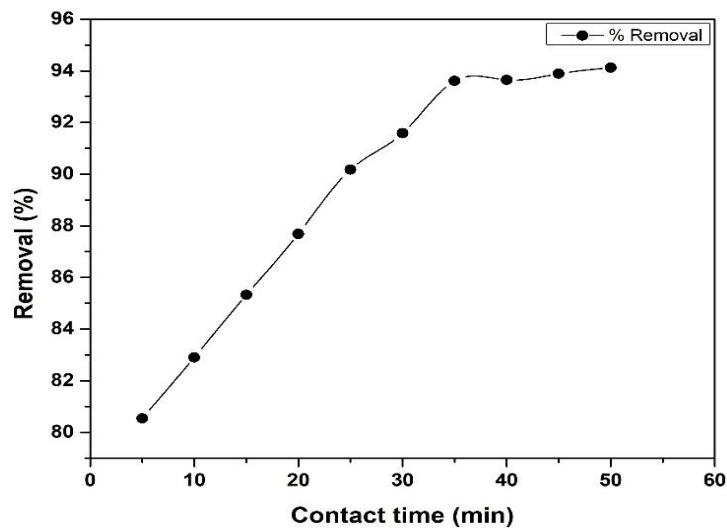


Figure 7: Effect of contact time

### 5.4 Effect of pH on percentage removal of Ni (II) using Fe<sub>3</sub>O<sub>4</sub> nanoparticle as adsorbent

One of the key factors influencing the adsorbent's ability to absorb Ni(II) ions from aqueous solutions is pH. The synthetic nanoFe<sub>3</sub>O<sub>4</sub>'s adsorption potential was determined at different pH values (3–8) while maintaining the system under the following conditions: The Fe<sub>3</sub>O<sub>4</sub> nanoparticle dose (0.4 g), initial metal ion concentration (40 ppm), and contact time (35 min) were all fixed. The synthesised nanoFe<sub>3</sub>O<sub>4</sub> was found to be effective in removing the Ni(II) ion only in acidic media, with a pH range of 6. This observation indicates that the adsorption process relies on pH[13,14,17].

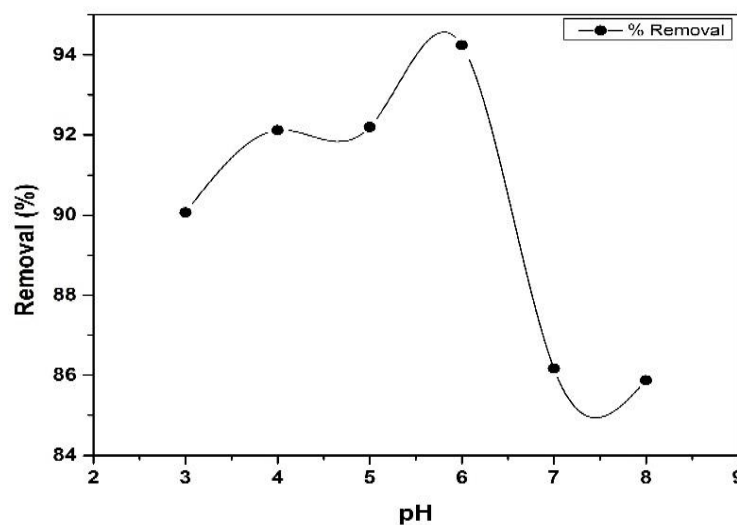


Figure 8: Effect of pH

### 6. Adsorption isotherm

Figure 9: Langmuir isotherm model

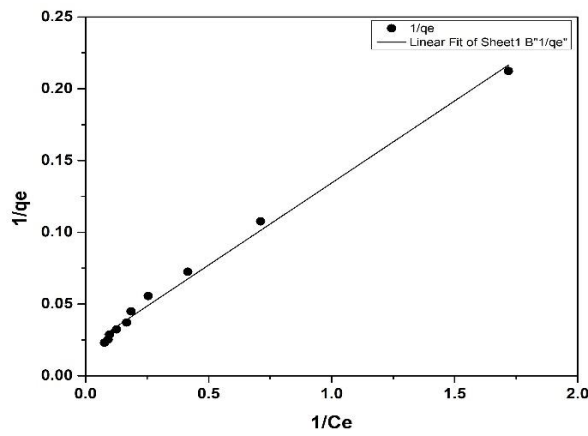


Table 1: Langmuir adsorption parameters

<b>Intercept</b>	0.01994
<b>Slope</b>	0.11438
<b>q<sub>max</sub>(mg/g)</b>	50.15045135
<b>K<sub>L</sub></b>	0.174331177
<b>R<sub>L</sub></b>	0.125419
<b>R<sup>2</sup></b>	0.99221

Figure 10: Freundlich isotherm model

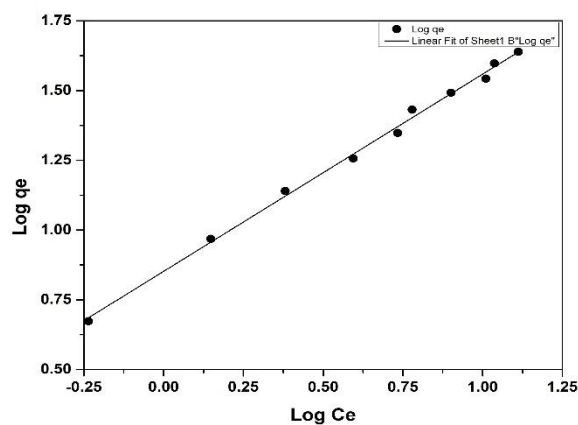


Table 2: Freundlich adsorption parameters

<b>Intercept</b>	0.85175
<b>Slope</b>	0.70706
<b>1/n</b>	0.70706
<b>K<sub>f</sub></b>	7.108042
<b>R<sup>2</sup></b>	0.9961

The experimental adsorption equilibrium data were analysed using two adsorption models, such as the Langmuir and Freundlich models (Figures 9 and 10) in their formats, to look into the mechanism of



adsorption onto synthetic ferric oxide nanoparticles[18,19]. The correlated constants (tables no. 1 and 2) are calculated from the slopes and intercepts of these models. After the study data was fitted to both isotherm models and the higher correlation coefficient values ( $R^2 \sim 1$ ) were taken into consideration, it was determined that the Freundlich and Langmuir isotherm models offered the most precise explanation for the adsorption of nickel ions onto synthetic ferric oxide nanoparticles.

### 7. Adsorption kinetic

A variety of kinetic models, such as pseudo-first-order and pseudo-second-order models, were applied to evaluate the nickel ion adsorption kinetics onto the synthetic ferric oxide surface (Figures 11 and 12). The variable parameters (Tables Nos 3 and 4) were calculated using the plots of the kinetic model equation. The two models' primary application requirements are concordance between the computed and experimental values of  $q_e$  and the correlation coefficient ( $R^2$ ). The higher values of ( $R^2 \sim 1$ ) and almost identical experimental and estimated values of  $q_e$  (tables 3 and 4) suggest that the system behaves as if it were following a pseudo-second-order kinetic model.

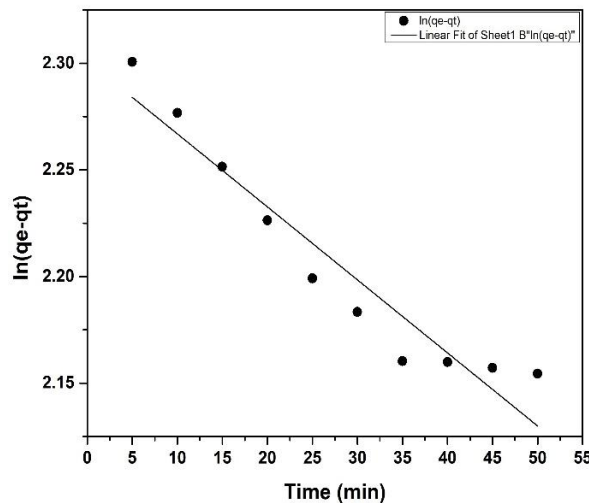


Figure 11: Pseudo first order

<b>Intercept</b>	2.30113
<b>Slope</b>	-0.00342
<b>qe(mg/g)</b>	9.98546
<b>K<sub>1</sub></b>	-0.000076
<b>R<sup>2</sup></b>	0.91144

Table 3: Pseudo first order parameters



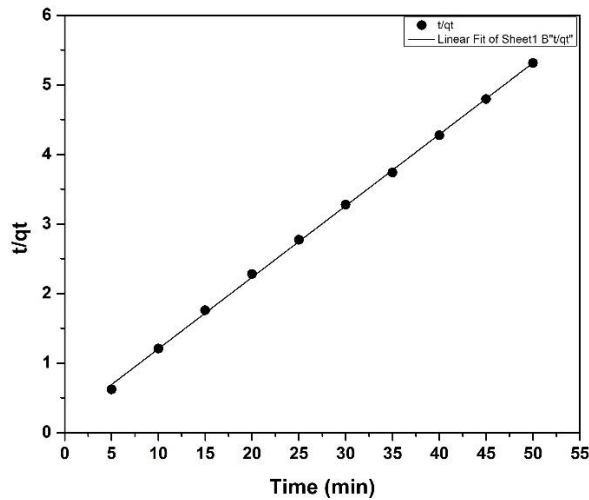


Figure 12: Pseudo second order

Intercept	0.17706
Slope	0.10276
$q_e$ (mg/g)	9.731413
$qe^2$	94.7004
$K_2$	0.059639
$R^2$	0.99942

Table 4: Pseudo second order parameters

### Conclusion

In this investigation, an appropriate native nanomaterial prepared using a modified sol-gel process has been found to be a useful adsorbent for the adsorption of Ni(II) ions from synthetic aqueous solutions. With an optimal Ni(II) ion concentration of 50 ppm, an adsorbent dosage of 0.4 g, and a pH of 6, the results showed that the adsorption process achieved equilibrium in 40 minutes and that 94% of the Ni(II) ions were removed during this period. Ni(II) adsorption kinetics on Fe<sub>3</sub>O<sub>4</sub> nanomaterials were found to match the pseudo second order model, according to the kinetic data. Both the Freundlich and the Langmuir isotherms provided a good fit for the adsorption data. According to these findings, Fe<sub>3</sub>O<sub>4</sub> nanoparticles can be employed as an excellent adsorbent in the purification of water since they are very effective at removing the Ni(II) cation from aqueous media.

### References

1. D. Chen, T. Awut, B. Liu, Y. Ma, T. Wang, and I. Nurulla, “Functionalized magnetic Fe<sub>3</sub>O<sub>4</sub> nanoparticles for removal of heavy metal ions from aqueous solutions,” *e-Polymers*, vol. 16, no. 4, pp. 313–322, Jul. 2016, doi: 10.1515/epoly-2016-0043.
2. J. S. Kwon, S. T. Yun, J. H. Lee, S. O. Kim, and H. Y. Jo, “Removal of divalent heavy metals (Cd, Cu, Pb, and Zn) and arsenic(III) from aqueous solutions using scoria: Kinetics and equilibria of sorption,” *J Hazard Mater*, vol. 174, no. 1–3, pp. 307–313, Feb. 2010, doi: 10.1016/j.jhazmat.2009.09.052.

3. L. Carlos, F. S. Garcia Einschlag, M. C., and D. O., "Applications of Magnetite Nanoparticles for Heavy Metal Removal from Wastewater," in *Waste Water - Treatment Technologies and Recent Analytical Developments*, InTech, 2013. doi: 10.5772/54608.
4. M. Hadadian, E. K. Goharshadi, M. M. Fard, and H. Ahmadzadeh, "Synergistic effect of graphene nanosheets and zinc oxide nanoparticles for effective adsorption of Ni (II) ions from aqueous solutions," *Appl Phys A Mater Sci Process*, vol. 124, no. 3, Mar. 2018, doi: 10.1007/s00339-018-1664-8.
5. S. Lang~rd, "Nickel-related cancer in welders," 1994.
6. M. Hossain, M. Hossain, M. Begum, M. Shahjahan, M. Islam, and B. Saha, "Magnetite (Fe<sub>3</sub>O<sub>4</sub>) nanoparticles for chromium removal," *Bangladesh Journal of Scientific and Industrial Research*, vol. 53, no. 3, pp. 219–224, Sep. 2018, doi: 10.3329/bjsir.v53i3.38269.
7. Z. N. Kayani, S. Arshad, S. Riaz, and S. Naseem, "Synthesis of Iron Oxide Nanoparticles by Sol–Gel Technique and Their Characterization," *IEEE Trans Magn*, vol. 50, no. 8, pp. 1–4, Aug. 2014, doi: 10.1109/TMAG.2014.2313763.
8. S. Shaker *et al.*, "Synthesis of Magnetite Nanoparticles by Sol-Gel Method for Environmental Applications Preparation And Characterization Of Magnetite Nanoparticles By Sol-Gel Method For Water Treatment," *Int J Innov Res Sci Eng Technol*, vol. 2, 2013, [Online]. Available: [www.ijirset.com](http://www.ijirset.com)
9. R. Ansari, Z. Esdaki, and F. Ostovar, "Synthesis, characterization, and application of polypyrrole/Fe<sub>3</sub>O<sub>4</sub> nanocomposite for removal of Ni(II) ions from water and wastewaters," *Polymer Bulletin*, vol. 80, no. 9, pp. 9451–9464, Sep. 2023, doi: 10.1007/s00289-022-04493-8.
10. D. Chen, T. Awut, B. Liu, Y. Ma, T. Wang, and I. Nurulla, "Functionalized magnetic Fe<sub>3</sub>O<sub>4</sub> nanoparticles for removal of heavy metal ions from aqueous solutions," *E-Polymers*, vol. 16, no. 4, pp. 313–322, Jul. 2016, doi: 10.1515/epoly-2016-0043.
11. M. Hossain, M. Hossain, M. Begum, M. Shahjahan, M. Islam, and B. Saha, "Magnetite (Fe<sub>3</sub>O<sub>4</sub>) nanoparticles for chromium removal," *Bangladesh Journal of Scientific and Industrial Research*, vol. 53, no. 3, pp. 219–224, Sep. 2018, doi: 10.3329/bjsir.v53i3.38269.
12. Z. N. Kayani, S. Arshad, S. Riaz, and S. Naseem, "Synthesis of Iron Oxide Nanoparticles by Sol-Gel Technique and Their Characterization," *IEEE Trans Magn*, vol. 50, no. 8, Aug. 2014, doi: 10.1109/TMAG.2014.2313763.
13. S. Shaker *et al.*, "Synthesis of Magnetite Nanoparticles by Sol-Gel Method for Environmental Applications preparation and characterization of magnetite nanoparticles by sol-gel method for water treatment," *Int J Innov Res Sci Eng Technol*, vol. 2, 2013, [Online]. Available: [www.ijirset.com](http://www.ijirset.com)
14. R. Ansari, Z. Esdaki, and F. Ostovar, "Synthesis, characterization, and application of polypyrrole/Fe<sub>3</sub>O<sub>4</sub> nanocomposite for removal of Ni(II) ions from water and wastewaters," *Polymer Bulletin*, vol. 80, no. 9, pp. 9451–9464, Sep. 2023, doi: 10.1007/s00289-022-04493-8.
15. Y. C. Sharma and V. Srivastava, "Separation of Ni(II) ions from aqueous solutions by magnetic nanoparticles," *J Chem Eng Data*, vol. 55, no. 3, pp. 1441–1442, Mar. 2010, doi: 10.1021/je900619d.
16. Y. C. Sharma, V. Srivastava, C. H. Weng, and S. N. Upadhyay, "Removal of Cr(VI) from wastewater by adsorption on iron nanoparticles," *Canadian Journal of Chemical Engineering*, vol. 87, no. 6, pp. 921–929, Dec. 2009, doi: 10.1002/cjce.20230.
17. Z. N. Kayani, S. Arshad, S. Riaz, and S. Naseem, "Synthesis of Iron Oxide Nanoparticles by Sol-Gel Technique and Their Characterization," *IEEE Trans Magn*, vol. 50, no. 8, Aug. 2014, doi: 10.1109/TMAG.2014.2313763.

18. P. Panneerselvam, N. Morad, and K. A. Tan, “Magnetic nanoparticle (F<sub>3</sub>O<sub>4</sub>) impregnated onto tea waste for the removal of nickel(II) from aqueous solution,” *J Hazard Mater*, vol. 186, no. 1, pp. 160–168, Feb. 2011, doi: 10.1016/j.jhazmat.2010.10.102.
19. I. Langmuir and B. Irving Langmuir, “I 848 [contribution from the research laboratory of the general electric com-the constitution and fundamental properties of solids and liquids. 11. Liquids.’.”